Inorganic Chemistry

ARTICLE

pubs.acs.org/IC

Stabilizing High-Valent Metal Ions with a Ketimide Ligand Set: Synthesis of $Mn(N{=}C^tBu_2)_4$

Richard A. Lewis, Guang Wu, and Trevor W. Hayton*

Department of Chemistry and Biochemistry, University of California Santa Barbara, Santa Barbara California 93106, United States

Supporting Information

ABSTRACT:

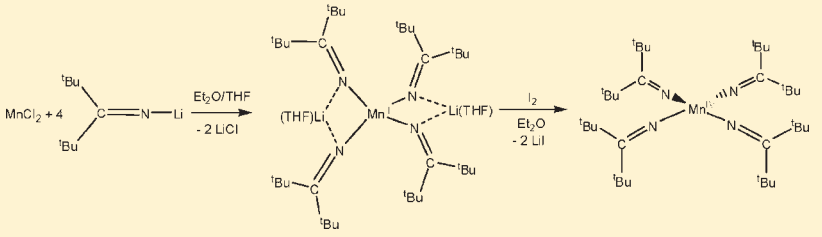

Reaction of $MnCl_2$ with 4 equiv of $Li(N{=}C^tBu_2)$ generates $[Li(THF)]_2[Mn(N{=}C^tBu_2)_4]$ (**1**) in 80% yield. Oxidation of **1** with 0.5 equiv of I_2 produces $[Li][Mn(N{=}C^tBu_2)_4]$ (**2**) in 88% yield. Both complexes **1** and **2** exhibit tetrahedral structures about the Mn center in the solid-state, as determined by X-ray crystallography. Reaction of **2** with 12-crown-4 generates $[Li(12\text{-crown-}4)_2][Mn(N{=}C^tBu_2)_4]$ (**3**) in 94% yield. Interestingly, in the solid-state, complex **3** exhibits a squashed tetrahedral structure about Mn. Addition of 1 equiv of I_2 to **1** generates the Mn(IV) ketimide, $Mn(N{=}C^tBu_2)_4$ (**4**), in 75% yield. Complex **4** was fully characterized, including analysis by X-ray crystallography and cyclic voltammetry. Like **3**, complex **4** also exhibits a squashed tetrahedral structure in the solid-state. Interestingly, thermolysis of complex **4** at 50 °C for 6 h results in the formation of $Mn_3(N{=}C^tBu_2)_6$ (**6**), which can be isolated in 49% yield. Also observed in the reaction mixture is pivalonitrile, isobutylene, and isobutene, the products of ketimide ligand oxidation. We have also synthesized the homoleptic Cr(IV) ketimide complex, $Cr(N{=}C^tBu_2)_4$ (**5**), and have analyzed its electrochemical properties with cyclic voltammetry.

INTRODUCTION

High valent manganese is of interest because of its role in oxygen evolution by Photosystem II,[1−3] and also because of its proposed intermediacy in numerous synthetically relevant oxidations.[4−7] In this regard, a variety of coligands have been interrogated for their ability to stabilize the 4+ and 5+ oxidation states of Mn, including, most prominently, porphyrins and corroles.[6−12] Amides have also proven useful at stabilizing Mn(IV),[13] such as the tripodal $[H_3buea]^{3-}$ ligand ($[H_3buea]^{3-}$ = tris[(*N*′-*tert*-butylureaylato)-*N*-ethylene]aminato), used to stabilize a terminal oxo complex of Mn^{4+}.[14−18] Additionally, Collins and co-workers have reported the synthesis of several high valent Mn complexes ligated by a tetra(amido) macrocyclic ligand,[19−21] while several high valent Mn ions ligated by mixed bis(amido)/bis(alkoxo) ligands are also known.[22−24] Aryloxide ligands are also capable of supporting high-valent manganese.[25−27] Of these, iminophenolate-containing ligands are most prevalent,[28−30] as illustrated in the Mn(IV) complex $[Mn(SALPN)O]_2$ (SALPN = 1,3-bis(salicylideneamino)propane).[30,31] Finally, the synthesis of a homoleptic M(IV) alkyl complex, $Mn(norbornyl)_4$, has been reported, but this material has not been fully characterized.[32]

Despite these advances, however, Mn(IV) alkoxo and amido complexes are still relatively rare. For example, to our knowledge, neither a homoleptic Mn(IV) amide nor homoleptic Mn(IV) alkoxide is known. This is remarkable, given the importance of these two ligand sets to modern coordination chemistry,[33,34] and reveals the acute challenge in generating and isolating high-valent manganese coordination complexes. It also reveals the need to identify new ligands sets capable of supporting Mn^{4+}. In this regard, we recently reported the synthesis of a stable Fe(IV) ketimide complex, namely, $Fe(N{=}C^tBu_2)_4$.[35] Interestingly, this complex exhibits a diamagnetic ground state and a square planar geometry. The utility of $[N{=}C^tBu_2]^-$ at stabilizing M^{4+} ions was further illustrated by the recent isolation of $Cr(N{=}C^tBu_2)_4$ by Hoffman and co-workers.[36] Again, this complex is diamagnetic, but in contrast to the Fe analogue, it exhibits a D_{2d} geometry. The unique structures and electronic properties exhibited by these two complexes have motivated us to further explore the coordination chemistry of the ketimide ligand. Herein we report the synthesis and characterization of a homoleptic Mn(IV) ketimide complex and analyze the emerging structural trends observed for the $M(N{=}C^tBu_2)_4$ series.

RESULTS AND DISCUSSION

The addition of 4 equiv of $Li(N{=}C^tBu_2)$ to $MnCl_2$, in THF, yields a bright yellow solution. Filtration of the reaction mixture

Received: March 9, 2011
Published: April 12, 2011

Scheme 1

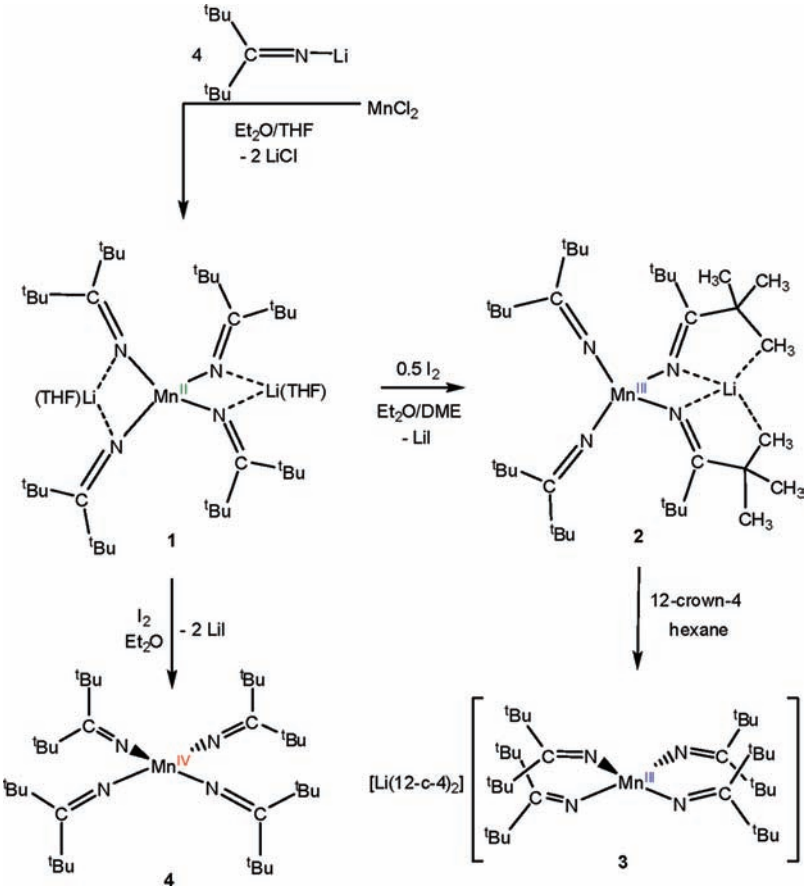

and recrystallization from a concentrated Et_2O solution yields $[Li(THF)]_2[Mn(N{=}C^tBu_2)_4]$ (**1**), as a yellow powder in 80% yield (Scheme 1).

Single crystals suitable for X-ray diffraction analysis were obtained from a dilute hexane solution stored at −25 °C. In the solid state, **1** crystallizes in the monoclinic space group $P2_1/n$ and exhibits a distorted tetrahedral geometry about Mn (Figure 1). Complex **1** is isostructural with the Fe analogue,[35] but, as expected, the Mn−N bond lengths are slightly longer than the Fe−N bond lengths, consistent with the presence of the larger Mn^{2+} ion. In particular, the Mn−N bond lengths range from Mn1−N4 = 2.107(3) Å to Mn1−N3 = 2.118(3) Å. These bond lengths are comparable to the Mn−N bond lengths found in manganese amides.[37] In addition, there are two Li cations contained within the secondary coordination sphere of **1**. Each cation is coordinated by two ketimide nitrogen atoms, one THF molecule, and by agostic interactions with two ketimide methyl groups.[38]

The ^{1}H NMR spectrum of **1** in C_6D_6 consists of an extremely broad singlet at 17.3 ppm, which we have assigned to the *tert*-butyl groups of the ketimide ligands. In addition, two broad resonances are observed at 3.5 ppm and 1.3 ppm, which are assignable to THF. No resonance is observed in the ^{7}Li{^{1}H} NMR spectrum. The magnetic susceptibility of **1** at 300 K was determined to be 5.98 μ_B by SQUID magnetometry (Figure 2). This is within the range expected for an $S = 5/2$ ground state, and is consistent with the presence of a high spin d^5 ion.[39]

Complex **1** is readily oxidized by addition of 0.5 equiv of I_2 to yield a dark brown solution, from which $[Li][Mn(N{=}C^tBu_2)_4]$ (**2**) can be isolated as a deep brown crystalline solid in good yield (Scheme 1). Its ^{1}H NMR spectrum in C_6D_6 consists of a broad singlet at 9.1 ppm, which we have assigned to the *tert*-butyl groups of the ketimide ligand, while the ^{7}Li{^{1}H} NMR spectrum exhibits a broad resonance at 85.3 ppm.

Complex **2** crystallizes in the orthorhombic space group *Pnna*, and exhibits a tetrahedral geometry about the Mn ion (e.g., N1−Mn1−N2 = 107.64(14)°, N1−Mn1−N1* = 113.3(2)°, N2−Mn1−N2* = 114.1(2)°) (Figure 3). In the solid state, complex **2** contains a single Li cation contained within its secondary coordination sphere. However, the Li cation is disordered over two sites, namely, the binding site defined by N1 and N1* and the binding site defined by N2 and N2*. Each site was modeled with half occupancy. In both sites the cation interacts with two ketimide nitrogen atoms and two methyl groups of the *tert*-butyl substituents, in a roughly square planar arrangement. A similar interaction has been observed previously in the solid-state molecular structure of $[Li][Al(N{=}C^tBu_2)_4]$.[40] While disorder was detected for the Li^+ cation, alternate positions for the ketimide ligands were not observed. Thus the metrical parameters of the ketimides represent an average of the bridging and terminal coordination modes. Nonetheless, the Mn−N bond lengths (Mn1−N1 = 1.902(3) Å and Mn1−N2 = 1.900(4) Å) are shorter than those observed for complex **1**, consistent with the combined influence of the smaller Mn^{3+} ion and the presence of two terminal ketimide ligands.

Interestingly, complex **2** is not isostructural with its isoelectronic d^4 iron analogue, $Fe(N{=}C^tBu_2)_4$.[35] We reasoned that the

dx.doi.org/10.1021/ic200490v |*Inorg. Chem.* 2011, 50, 4660–4668

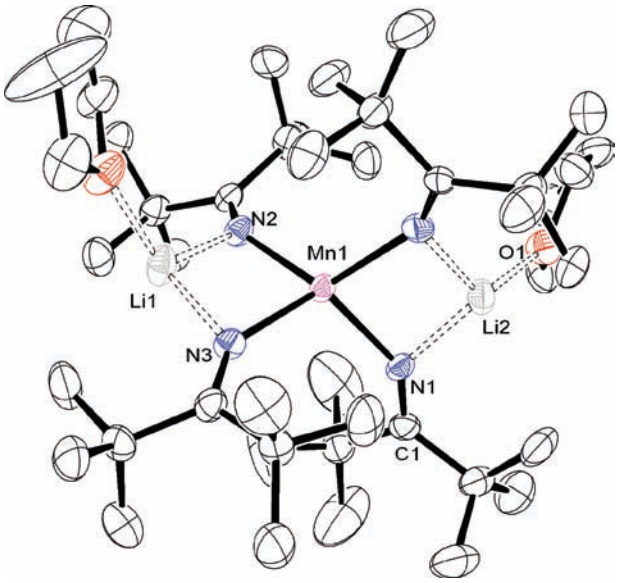

Figure 1. ORTEP diagram of $[Li(THF)]_2[Mn(N{=}C^tBu_2)_4]$ (**1**) with 50% probability ellipsoids. Selected bond lengths (Å) and bond angles (deg): Mn1−N1 = 2.114(3), Mn1−N2 = 2.117(3), Mn1−N3 = 2.118(3), Mn1−N4 = 2.107(3), N1−Li2 = 1.961(7), N4−Li2 = 1.978(7), N3−Li1 = 1.975(7), N2−Li1 = 1.984(7), N1−C1 = 1.249(5), Li2−O1 = 1.973(7), N4−Mn1−N1 = 92.37(12), N2−Mn1−N1 = 119.53(11), Mn1−N1−C1 = 145.4(3).

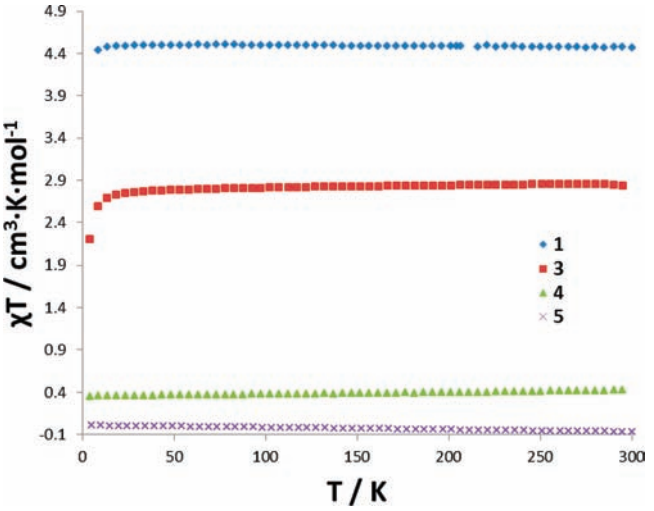

Figure 2. Temperature dependent magnetic susceptibility of complexes **1**, **3**, **4**, and **5**.

aforementioned Li cation was perturbing the complex away from the preferred square planar arrangement. Given this consideration we attempted to sequester the Li ion in **2** with 12-crown-4, so as to compare the structures and electronic properties of two truly isostructural $[M(N{=}C^tBu_2)_4]^{0/-}$ (M = Mn, Fe) complexes. Thus, layering a hexane solution of 12-crown-4 upon an Et_2O solution of **2**, followed by storage at −25 °C, provides $[Li(12\text{-crown-}4)_2][Mn(N{=}C^tBu_2)_4]$ (**3**) as dark purple solid in good yield (Scheme 1).

Complex **3** crystallizes in the triclinic space group $P\bar{1}$ as a discrete cation/anion pair (Figure 4). Its Mn−N bond lengths range from 1.888(4) Å to 1.913(3) Å, and are comparable to the

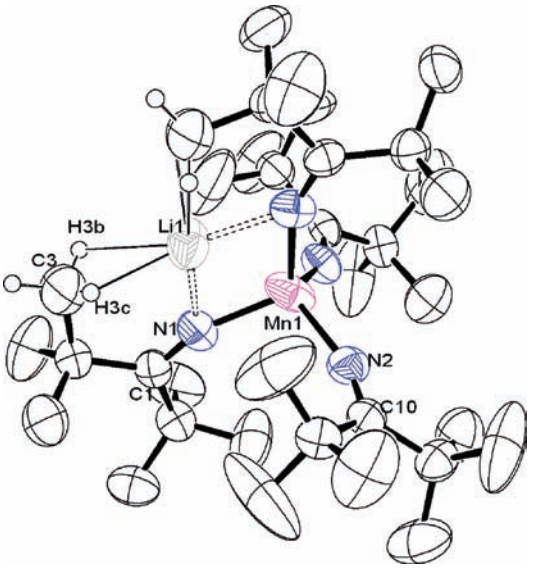

Figure 3. ORTEP diagram of $[Li][Mn(N{=}C^tBu_2)_4]$ (**2**) with 50% probability ellipsoids. Selected bond lengths (Å) and bond angles (deg): Mn1−N1 = 1.902(3), Mn1−N2 = 1.900(4), Li1−N1 = 2.022(15), N1−Mn1−N2 = 107.64(14), N1−Mn1−N1* = 113.3(2), Mn1−N1−C1 = 154.7(3), Mn1−N2−C10 = 157.5(3).

Mn−N bond lengths observed in **2**. The Mn center in complex **3** exhibits a distorted square planar geometry, much different than the tetrahedral geometry observed in **2**. For example, the largest N−Mn−N angles are N1−Mn1−N3 = 143.60(15)° and N2−Mn1−N4 = 143.47(15)°. These values are notably smaller than those observed for the isoelectronic Fe(IV) complex, $Fe(N{=}C^tBu_2)_4$ (N1−Fe1−N1* = 167.1(2)°; N2−Fe1−N2* = 167.6(2)°).[35] In addition, the four ketimide ligands in **3** are not coordinated in a linear fashion, as was observed in the Fe(IV) analogue. In particular, the Mn−N−C angles range from 149.8(3)° to 153.0(3)°. This change in coordination behavior is likely due to the high-spin nature of complex **3** (vide infra), which reduces the ability of the ketimide ligand to act as a π-donor because of unfavorable electron−electron repulsions between the partially filled d orbitals and the nitrogen lone pairs. Several other four coordinate d^4 complexes,[41] such as $[Li(THF)_2]_2[CrPh_4]$, $[Li(TMEDA)]_2[CrMe_4]$, and $[Li(TMEDA)_2][MnMe_4]$,[42−44] also exhibit nontetrahedral geometries. For example, $[Li(TMEDA)_2][MnMe_4]$ exhibits a distorted square planar geometry about Mn, with the largest C−Mn−C bond angles being 160.8(2)° and 161.8(2)°.

The ^1H NMR spectrum of **3** in pyridine-d_5 consists of a broad singlet at 12.4 ppm, which we have assigned to the *tert*-butyl groups of the ketimide ligand. Additionally, we observe a sharp singlet at 3.66 ppm, assignable to the methylene protons of the $[Li(12\text{-crown-}4)_2]$ cation. The $^7Li\{^1H\}$ NMR spectrum in pyridine-d_5 consists of a singlet at 3.54 ppm. The solid state magnetic susceptibility of **3**, at 300 K, yields an effective magnetic moment of 4.74 μ_B, which is consistent with the $S = 2$ ground state expected for a high-spin d^4 ion (Figure 2).[45,46] This contrasts with the low spin, $S = 0$ ground state observed for its isoelectronic Fe(IV) analogue.[35] We attribute this difference to the disparity in charge between the 3+ ion in **3** and the 4+ ion in the Fe complex. The higher charge in the Fe example leads to a greater ligand field splitting and results in a low spin ground state.

dx.doi.org/10.1021/ic200490v |*Inorg. Chem.* 2011, 50, 4660–4668

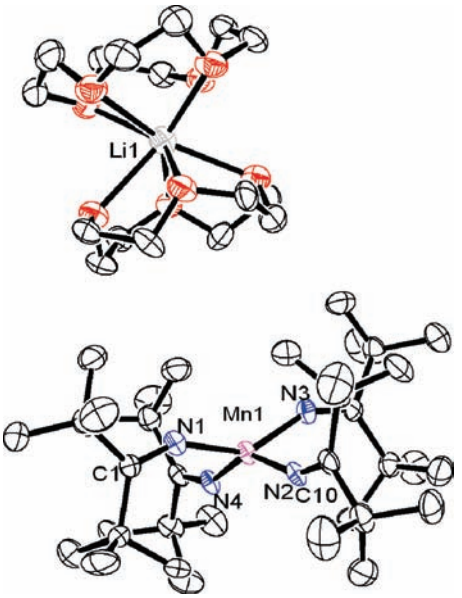

Figure 4. ORTEP diagram of $[Li(12\text{-crown-}4)_2][Mn(N{=}C^tBu_2)_4]$ (**3**) with 50% probability ellipsoids. Selected bond lengths (Å) and bond angles (deg): Mn1−N1 = 1.913(3), Mn1−N2 = 1.888(4), Mn1−N3 = 1.903(3), Mn1−N4 = 1.895(3), N1−C1 = 1.264(5), Li1−O1 = 2.373(9), N1−Mn1−N2 = 95.16(14), N1−Mn1−N3 = 143.60(15), Mn1−N1−C1 = 149.8(3), Mn1−N2−C10 = 153.0(3).

Complex **3** is stable in DME or pyridine. However, it appears to react with both dichloromethane and acetonitrile. In the case of the former, dissolution results in the formation of complex **4** (vide infra), as determined by ^{1}H NMR spectroscopy. In the case of the latter, dissolution only yields an intractable solid. Interestingly, the sequestration of the Li cation in complex **3** appears to be reversible. Dissolution of **3** in C_6D_6 results in the formation of a deep yellow-brown solution, quite different from the purple solutions typically associated with this material. The ^{1}H NMR spectra of these solutions are consistent with presence of complex **2** and free 12-crown-4. The low dielectric constant of benzene, versus that of DME or pyridine, likely destabilizes the cation/anion pair found in **3** and promotes reformation of **2**.

Complex **1** is also readily oxidized by two electrons. Thus, addition of 1 equiv of I_2 to **1** in Et_2O yields a dark red-orange solution, from which $Mn(N{=}C^tBu_2)_4$ (**4**) can be isolated as a red-orange crystalline solid in good yield (Scheme 1). The ^{1}H NMR spectrum of **4** in C_6D_6 consists of a singlet centered at 5.10 ppm, assignable to the *tert*-butyl groups on the ketimide ligands. The solid state magnetic susceptibility of **4** was determined to be 1.85 μ_B at 300 K (Figure 2), which is consistent with an $S = 1/2$ ground state of a low spin d^3 ion.[47] This spin state is also in-line with the low spin electronic configurations observed for the Cr and Fe analogues.[35,36]

Crystals of **4** suitable for X-ray diffraction were obtained by storage in a concentrated pentane solution at −25 °C for 24 h. Complex **4** crystallizes in the triclinic space group $P\bar{1}$, and as observed for complex **3**, it exhibits a distorted square planar geometry about Mn (Figure 5). For example, the largest N−Mn−N bond angles (N2−Mn1−N4 = 151.12(12)° and N1−Mn1−N3 = 150.31(12)°) are nearly identical to the largest N−Mn−N angles observed for **3**. Additionally, the Mn−N bond lengths range from 1.781(3) Å to 1.790(3) Å, which is about 0.1 Å shorter than the Mn−N bond lengths observed in **3**, consistent

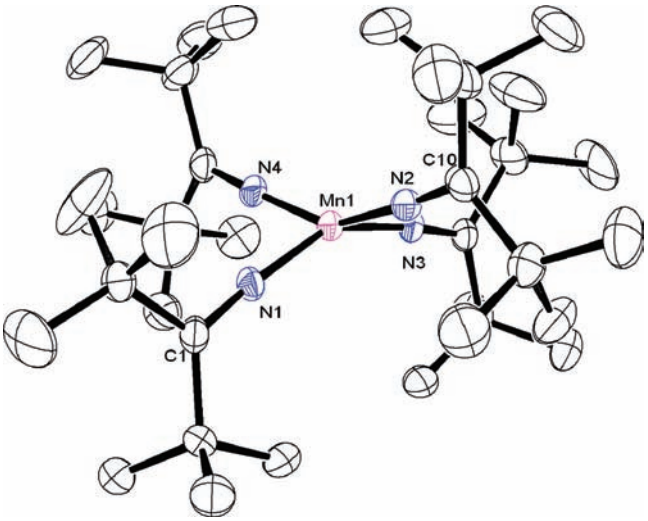

Figure 5. ORTEP diagram of $Mn(N{=}C^tBu_2)_4$ (**4**) with 50% probability ellipsoids. Selected bond lengths (Å) and bond angles (deg): Mn1−N1 = 1.790(3), Mn1−N2 = 1.782(3), Mn1−N3 = 1.781(3), Mn1−N4 = 1.786(3), N1−C1 = 1.259(4), N1−Mn1−N2 = 93.90(12), N1−Mn1−N3 = 150.31(12), Mn1−N1−C1 = 174.1(2), Mn1−N4−C28 = 177.6(2), N2−Mn1−N4 = 151.12(12).

with oxidation from Mn(III) to Mn(IV). Unlike complex **3**, however, the four ketimide ligands in **4** are ligated in a linear fashion (e.g., Mn1−N1−C1 = 174.1(2)°, Mn1−N4−C28 = 177.6(2)°). We attribute this change to the low spin configuration of **4**, which allows for greater π-donation from the ketimide ligands.

Complex **4** is the fourth homoleptic M^{4+} ketimide complex to be structurally characterized for the first row transition metals. Its characterization allows for the opportunity to compare the structural features of this unique series of M(IV) complexes. A selection of metrical parameters for these four complexes is shown in Table 1. Most interesting is the correlation between the coordination geometry and the d electron count of the metal ion. Specifically, as the d count of the metal ion increases from zero (Ti) to four (Fe), the geometry about the metal ion changes gradually from tetrahedral (Ti, $\tau_4 = 0.99$) to square planar (Fe, $\tau_4 = 0.18$), where a τ_4 of 1 indicates an idealized tetrahedron and a τ_4 of 0 indicates an idealized square plane.[48] Accordingly, the Cr and Mn analogues both exhibit D_{2d} structures, with the Mn analogue being slightly closer to an idealized square plane than the Cr analogue. Hoffman and co-workers recently argued that the D_{2d} structure of $Cr(N{=}C^tBu_2)_4$ arises from the competing effects of π-donation from the ketimide ligands into the empty d_{z^2} orbital and π-back-donation from the filled d_{xy} orbital into the empty ketimide C=N π^* orbitals.[36] The π-donation interaction promotes a tetrahedral geometry, while the π-back-donation interaction promotes a square planar geometry. A similar explanation may also account for the D_{2d} and D_{4h} structures of complex **4** and $Fe(N{=}C^tBu_2)_4$, respectively. In these two complexes, the d_{z^2} orbital would be either partially (in **4**) or fully (in $Fe(N{=}C^tBu_2)_4$) occupied, reducing the T_d-promoting π-donation interaction and favoring a flattened structure. However, the π-donation/π-back-donation argument does not as readily rationalize the D_{2d} geometry of complex **3**, as the ketimide π-donor/π-acceptor capacity is presumably attenuated by the acute Mn−N−C angles. As an alternate explanation we propose that both **3** and **4** derive an increased crystal field stabilization by

dx.doi.org/10.1021/ic200490v |*Inorg. Chem.* 2011, 50, 4660–4668

Table 1. Comparison of the Metrical Parameters for $M(N{=}C^tBu_2)_4$ (M = Ti, Cr, Mn, Fe)

M	d count	M−N distances (Å)	M−N−C angles (deg)	N−M−N angles (deg)[a]	τ_4[b]	ref.
Ti	d^0	av. 1.87	av. 175	114.9 111.3	0.99	51
Cr	d^2	1.784(2) 1.785(2)	178.4(2) 179.1(2)	136.1(1) 136.2(1)	0.62	36
Mn	d^3	av. 1.78	av. 176	151.12(12) 150.31(12)	0.42	this work
Fe	d^4	1.771(3) 1.775(3)	165.5(3) 166.6(3)	167.1(2) 167.6(2)	0.18	35

[a] Defined as the two largest N−M−N angles observed in the complex. [b] As defined in ref 48.

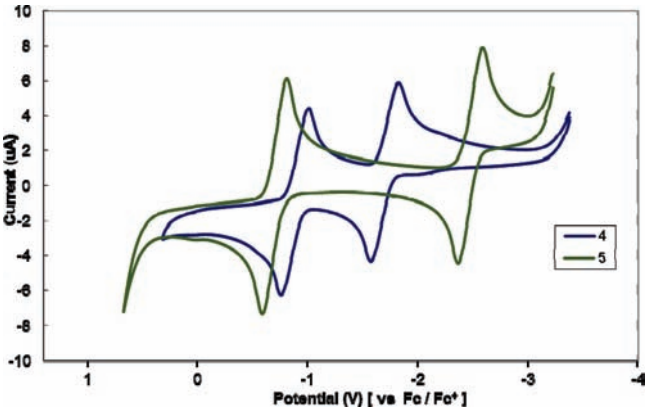

Figure 6. Cyclic voltammogram of complexes **4** and **5** (200 mV/s scan rate, vs Fc/Fc^+). Measured in THF with 0.1 M $[NBu_4][PF_6]$ as supporting electrolyte.

flattening to a D_{2d} structure.[49] This explanation also rationalizes the T_d geometry of $Ti(N{=}C^tBu_2)_4$, which would not exhibit any CFSE, and the nearly square planar geometry of $[Li(TMEDA)][MnMe_4]$,[44,50] for which the π-donation/π-back-donation argument does not apply, but which would still derive some CFSE by flattening to a square planar structure. Alternately, the D_{2d} geometry of complex **3** could be explained by the Jahn−Teller effect; however, this explanation is less likely for the low spin d^3 ion in complex **4**.[41] Nevertheless, CFSE or Jahn−Teller effects are not likely the only factors determining the structures of these complexes, as there is a competing steric effect which should favor the tetrahedral structure. The presence of counteracting steric and electronic effects may explain why the magnitude of flattening correlates with the d electron count.

The cyclic voltammogram of complex **4** in THF yields two reversible redox features at −1.67 V and −0.88 V (vs Fc/Fc^+) (Figure 6). The feature at −1.67 V is attributable to the Mn(II)/Mn(III) redox couple while the feature at −0.88 V is attributable to the Mn(III)/Mn(IV) redox couple. The Mn(III)/Mn(IV) redox potential is 0.35 V lower than the Fe(III)/Fe(IV) redox potential observed for $Fe(N{=}C^tBu_2)_4$,[35] consistent with the greater ability of Mn to achieve the 4+ oxidation state, relative to Fe.[52]

We have also synthesized the chromium analogue, $Cr(N{=}C^tBu_2)_4$ (**5**),[36] for comparison with complex **4**. Thus, addition of 4 equiv of $Li(N{=}C^tBu_2)$ to $CrCl_3$, followed by the addition of 0.5 equiv of I_2, yields a dark orange solution from which **5** can be isolated as dark orange blocks in 59% yield (eq 1). The $^{13}C\{^1H\}$ NMR spectrum of complex **5** reveals a resonance at 184.1 ppm, attributable to the α carbon of the ketimide ligand. Interestingly, this represents a 90 ppm upfield shift from the α carbon resonance of the iron analogue, $Fe(N{=}C^tBu_2)_4$.[35] We have also confirmed the diamagnetism reported by Hoffman using SQUID magnetometry (Figure 2).

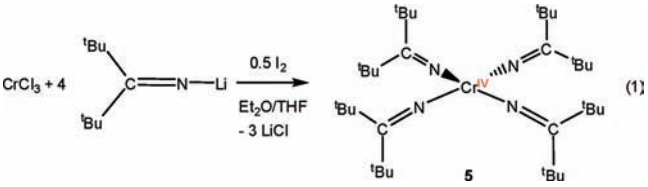

As was observed for complex **4**, the cyclic voltammogram of complex **5** yields two reversible redox features, at −2.48 V and −0.71 V (vs Fc/Fc^+) (Figure 6). The feature at −2.48 V is attributable to the Cr(II)/Cr(III) redox couple, while the feature at −0.71 V is attributable to the Cr(III)/Cr(IV) redox couple. As expected, the Cr(II)/Cr(III) redox potential is substantially lower than the Mn(II)/Mn(III) redox couple observed for **4**, consistent with the strong reducing power generally ascribed to Cr^{2+}.[53−55] In contrast, however, the M(III)/M(IV) redox potential for **5** is 0.17 V more positive than that observed for **4**. This may be a reflection of the relative instability of non-octahedral Cr^{3+} organometallics, previously noted during attempts to prepare homoleptic Cr(III) alkyls.[56]

Finally, we have begun exploring the reactivity of complex **4** to provide greater insight into the coordination chemistry of the high valent ketimides. Thermolysis of **4** at 50 °C for 6 h in C_6D_6 results in a striking color change from red-orange to yellow. From these solutions, $Mn_3(N{=}C^tBu_2)_6$ (**6**) can be isolated as yellow-brown crystalline solid in good yield (eq 2). Its ^1H NMR spectrum in C_6D_6 consists of two broad resonances at 17.1 ppm and 10.2 ppm, which we have assigned to the *tert*-butyl substituents of the terminal and bridging ketimide ligands, respectively. Complex **6** can also be prepared by reaction of $MnCl_2$ with 2 equiv of $Li(N{=}C^tBu_2)$ in THF, where it can be isolated in 50% yield.

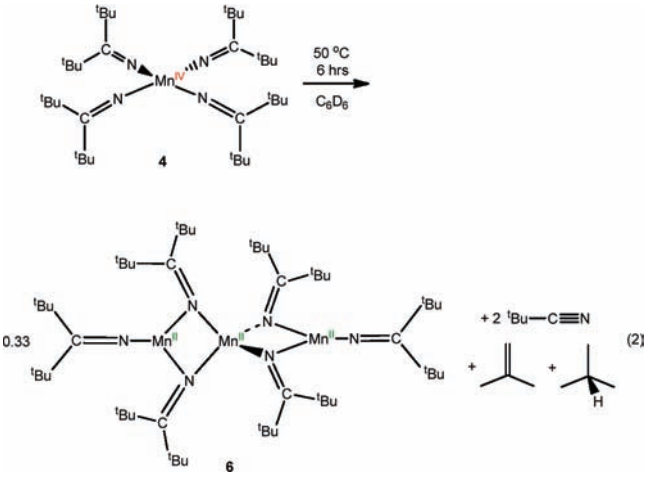

Crystals of **6** suitable for X-ray diffraction analysis were obtained from storage of a concentrated hexane solution at −25 °C for 24 h. Complex **6** crystallizes in the monoclinic space group *C*2/*c*,

dx.doi.org/10.1021/ic200490v |*Inorg. Chem.* 2011, 50, 4660–4668

and its solid-state molecular structure is shown in Figure 7. In the solid-state, complex **6** exists as a trimetallic cluster. The central manganese ion is coordinated by four ketimides, in an overall tetrahedral geometry, with Mn−N bond lengths of Mn1−N2 = 2.113(3) Å and Mn1−N3 = 2.120(3) Å. In addition, complex **6** contains two trigonal planar Mn ions, which are connected to the central Mn ion by two bridging ketimide ligands. Each trigonal planar Mn ion is also coordinated by one terminal ketimide ligand. The terminal ketimide ligand is coordinated in a linear fashion (Mn2−N1−C1 = 172.5(4)°), with an Mn−N bond length (Mn2−N1 = 1.885(4) Å) that is substantially shorter than those

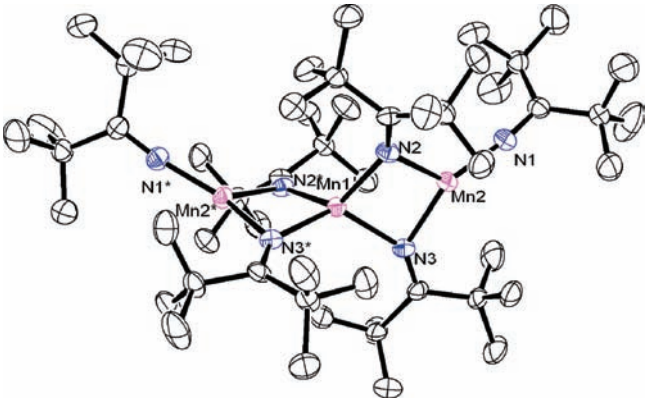

Figure 7. ORTEP diagram of $Mn_3(N{=}C^tBu_2)_2$ (**6**) with 50% probability ellipsoids. Asterisks indicate atoms generated by symmetry. Selected bond lengths (Å) and bond angles (deg): Mn1−N2 = 2.113(3), Mn1−N3 = 2.120(3), Mn2−N1 = 1.885(4), N1−C1 = 1.260(5), N1−Mn2−N2 = 122.57(15), N1−Mn2−N3 = 139.97(16), N2−Mn2−N3 = 94.75(14), N2−Mn1−N3* = 111.88(13).

exhibited by the bridging ketimides. Complex **6** is isostructural with several manganese alkoxides,[34] including $Mn_3(OCH^tBu_2)_6$.[57]

Monitoring the thermolysis of complex **4** in C_6D_6 by ^{1}H NMR spectroscopy reveals the formation of complex **6**, along with several new resonances between 0 ppm and 5 ppm. For example, resonances observed at 4.72 ppm and 1.57 ppm, in a 2:6 ratio, respectively, are consistent with the presence of isobutylene,[58] while broad resonances at 1.62 ppm and 0.83 ppm, in a 1:9 ratio, respectively, are consistent with the presence of isobutane.[59] Finally, a resonance observed at 0.75 ppm is consistent with the presence of pivalonitrile. These assignments are further supported by the ^{13}C-{^{1}H} NMR spectrum of the crude reaction mixture. For instance, resonances observed at 141.7 ppm, 110.8 ppm, and 23.8 ppm are assignable to isobutylene,[60] while resonances at 25.5 ppm and 24.5 ppm are assignable to isobutane.[61] Finally, resonances observed at 27.9 ppm and 27.5 ppm are assignable to the 1° and 3° butyl carbons, respectively, of pivalonitrile.[62] The presence of pivalonitrile in the reaction mixture was further confirmed by GC/MS. We also followed the thermolysis of complex **5** by ^{1}H NMR spectroscopy, but after 48 h at 50 °C, very little decomposition was observed.

The ^{1}H and ^{13}C{^{1}H} NMR data reveals that, upon thermolysis, the bis(*tert*-butyl)ketimide ligand is oxidized by the Mn^{4+} center, forming complex **6**, ^{t}BuCN, and presumably $Me_3C\cdot$ (eq 2), which then undergoes a well-established disproportionation to generate isobutylene and isobutane.[63−65] Two *tert*-butyl radicals can also combine to form 2,2,3,3-tetramethylbutane;[63−65] however, no evidence for the formation of this product is observed in the reaction mixture. The relative ease with which the ketimide ligand is oxidized most likely relates to the relatively high stability of the *tert*-butyl radical generated upon oxidation.[66]

Ketimides have previously been noted for their inertness, especially toward electrophilic attack and insertion of unsaturated

Table 2. X-ray Crystallographic Data for Complexes 1, 2, 3, 4, and 6

	1	2	3	4	6
empirical formula	$MnN_4C_{44}H_{88}O_2Li_2$	$MnN_4C_{36}H_{72}Li$	$MnN_4C_{52}H_{104}O_8Li$	$MnN_4C_{36}H_{72}$	$Mn_3N_6C_{54}H_{108}$
crystal habit, color	yellow, block	black, hexagon	purple, block	deep red, block	brown, block
crystal size (mm)	0.6 × 0.4 × 0.3	0.3 × 0.3 × 0.1	0.3 × 0.3 × 0.2	0.6 × 0.6 × 0.2	0.4 × 0.2 × 0.2
crystal system	monoclinic	orthorhombic	triclinic	triclinic	monoclinic
space group	$P2_1/n$	*Pnna*	$P\bar{1}$	$P\bar{1}$	$C2/c$
vol (Å^3)	4788(3)	4041.8(5)	2913.8(12)	1981.7(19)	5999.6(14)
a (Å)	12.638(4)	16.7762(12)	13.611(3)	11.356(6)	32.201(4)
b (Å)	19.844(7)	15.2054(10)	13.612(3)	11.738(6)	11.2776(15)
c (Å)	19.216(7)	15.8446(11)	16.360(4)	16.586(10)	22.819(3)
α (deg)	90.00	90.00	105.791(5)	70.20(2)	90.00
β (deg)	96.517(6)	90.00	92.476(5)	89.51(2)	133.615(2)
γ (deg)	90.00	90.00	90.013(5)	73.210(19)	90.00
Z	4	4	2	2	4
fw (g/mol)	774.00	622.8	975.27	615.92	1006.28
density (calcd) (Mg/m^3)	1.074	1.024	1.112	1.032	1.114
abs coeff (mm^{-1})	0.312	0.352	0.276	0.359	0.658
F_{000}	1708	1376	1072	682	2196
total no. reflections	31130	25658	24321	16650	24543
unique reflections	6906	2929	10977	7790	6175
R_{int}	0.0614	0.0976	0.1139	0.1604	0.1096
final *R* indices [$I > 2\sigma(I)$]	R1 = 0.0649	R1 = 0.064	R1 = 0.0678	R1 = 0.0660	R1 = 0.0624
	wR2 = 0.1570	wR2 = 0.1655	wR2 = 0.1410	wR2 = 0.1731	wR2 = 0.1262
largest diff peak and hole (e$^-$ Å^{-3})	0.797 and −0.337	0.432 and −0.747	0.506 and −0.675	0.566 and −0.584	1.129 and −0.740
GOF	1.173	1.028	0.930	1.010	1.010

dx.doi.org/10.1021/ic200490v |*Inorg. Chem.* 2011, 50, 4660–4668

substrates.[51,67−69] This property has made them useful coligands for olefin polymerization catalysts.[70] However, ketimide ligands are obviously susceptible to oxidation, as evidenced by the formation of complex **6**, but also by the intermediacy of ketimide complexes in the preparation of ketazines, $(R_2C{=}N)_2$, via oxidative coupling.[71−73]

CONCLUDING REMARKS

The isolation of $Mn(N{=}C^tBu_2)_4$ further reveals the unique ability of the bis(*tert*-butyl)ketimido ligand at supporting the 4+ oxidation state of the first row transition metals. Additionally, this ligand imparts unique electronic and structural features upon coordination to metal ions, as evidenced by the D_{2d} structures observed for $[Mn(N{=}C^tBu_2)_4]^-$ and $Mn(N{=}C^tBu_2)_4$. In addition, we have found that the bis(*tert*-butyl)ketimido ligand is prone to thermally induced oxidation. This observation suggests that the stabilization of higher valent metal ions, such as Mn^{5+}, will require a more judicious choice of substituents for the ketimide ligand, specifically one that balances the electron donating capacity of the two R groups, with the stability of the organic radical generated upon ketimide oxidation. Moving away from the *tert*-butyl substituents may improve the thermal stability of the resulting ketimide complexes. This should be easily achievable, as ketimide ligands with a wide variety of substituents are known,[74,75] allowing for the optimization of steric bulk, electron donating ability, and thermal stability.

EXPERIMENTAL SECTION

General Procedures. All reactions and subsequent manipulations were performed under anaerobic and anhydrous conditions either under high vacuum or an atmosphere of nitrogen or argon. Tetrahydrofuran (THF), hexane, diethyl ether, and toluene were dried using a Vacuum Atmospheres DRI-SOLV solvent purification system. C_6D_6, DME, and 12-crown-4 were dried over activated 4 Å molecular sieves for 24 h before use. $Li(N{=}C^tBu_2)$ was synthesized according to the previously reported procedure,[75,76] while all other reagents were purchased from commercial suppliers and used as received.

^1H, $^{13}C\{^1H\}$, and $^7Li\{^1H\}$ NMR spectra and Evans' method determinations[77] were recorded on a Varian UNITY INOVA 400 or Varian UNITY INOVA 500 spectrometer. ^1H and $^{13}C\{^1H\}$ NMR spectra are referenced to external $SiMe_4$ using the residual protio solvent peaks as internal standards (^1H NMR experiments) or the characteristic resonances of the solvent nuclei (^{13}C NMR experiments). $^7Li\{^1H\}$ spectra were referenced to external LiCl in D_2O. IR spectra were recorded on a Mattson Genesis FTIR spectrometer while UV−vis/NIR experiments were performed on a UV-3600 Shimadzu spectrophotometer. GC/MS analyses were performed with a Hewlett-Packard 5970B GC/MSD. Elemental analyses were performed by the Microanalytical Laboratory at UC Berkeley.

Cyclic Voltammetry (CV) Measurements. CV experiments were performed with a CH Instruments 600c Potentiostat, and the data were processed using CHI software (version 6.29). All experiments were performed in a glovebox using a 20 mL glass vial as the cell. The working electrode consisted of a platinum disk embedded in glass (2 mm diameter), the counter electrode was a platinum wire, and the reference electrode consisted of AgCl plated on Ag wire. Solutions employed during CV studies were typically 1 mM in the metal complex and 0.1 M in $[Bu_4N][PF_6]$. All potentials are reported versus the $[Cp_2Fe]^{0/+}$ couple. For all trials, $i_{p,a}/i_{p,c} = 1$ for the $[Cp_2Fe]^{0/+}$ couple, while $i_{p,c}$ increased linearly with the square root of the scan rate (i.e., $\sqrt{v}$). Redox couples which exhibited behavior similar to the $[Cp_2Fe]^{0/+}$ couple were thus considered reversible.

Magnetism Measurements. Magnetism data were recorded using a Quantum Design MPMS 5XL SQUID magnetometer. Complexes **1**, **3**, **4**, and **5** were analyzed using 30−55 mg of powdered crystalline material loaded into a NMR tube, which was subsequently flame-sealed. The solid was kept in place with ∼45 mg quartz wool packed on either side of the sample. The data was corrected for the contribution of the NMR tube holder and 90 mg of quartz wool. Data for complex **1** were collected using a 1 T field between 9 K and 300 K, while data for complexes **3** and **4** were collected using a 1 T field between 2 K and 300 K. The experiment for complex **5** was performed using a 3 T field between 4 K and 300 K. Diamagnetic corrections ($\chi_{dia} = -5.52 \times 10^{-4}$ cm^3·mol^{-1} for **1**, $\chi_{dia} = -6.89 \times 10^{-4}$ cm^3·mol^{-1} for **3**, $\chi_{dia} = -4.60 \times 10^{-4}$ cm^3·mol^{-1} for **4**, $\chi_{dia} = -4.44 \times 10^{-4}$ cm^3·mol^{-1} for **5**) were made using Pascal's constants.[78]

$[Li(THF)]_2[Mn(N{=}C(^tBu)_2)_4]$ (1). To a white suspension of $Li(N{=}C^tBu_2)$ (303 mg, 2.06 mmol) in THF (3 mL) was added $MnCl_2$ (62 mg, 0.49 mmol). The solution immediately turned orange-yellow. This solution was allowed to stir for 1 h, whereupon the solvent was removed in vacuo and Et_2O (5 mL) was added to the resulting yellow solid. This solution was filtered through a Celite column supported on glass wool (0.5 cm ×2 cm) and the volume of the solution was reduced in vacuo to 2 mL. Storage at −25 °C for 24 h resulted in the deposition of yellow powder, which was isolated by decanting off the supernatant (304 mg, 80% yield). Anal. Calcd for $MnN_4C_{44}H_{88}O_2Li_2$: C, 68.28; H, 11.46; N, 7.24. Found: C, 68.12; H, 11.84; N, 7.25. ^1H NMR (C_6D_6, 25 °C, 500 MHz): δ 17.3 (br s, CMe_3), 3.53 (br s, 8H, α-THF), 1.35 (br s, 8H, β-THF). UV−vis (C_7H_8, 3.0×10^{-4} M): 364 nm ($\varepsilon = 1600$ L·mol^{-1}·cm^{-1}), 450 nm ($\varepsilon = 1200$ L·mol^{-1}·cm^{-1}), 564 nm (sh, $\varepsilon = 370$ L·mol^{-1}·cm^{-1}), 672 nm (sh, $\varepsilon = 420$ L·mol^{-1}·cm^{-1}). IR (hexane, cm^{-1}): 1617(s), 1613(s).

$[Li][Mn(N{=}C^tBu_2)_4]$ (2). To a yellow solution of **1** (312 mg, 0.403 mmol) in Et_2O (4 mL) was added I_2 (50 mg, 0.197 mmol) in Et_2O (2 mL). The solution immediately turned dark yellow-brown. The reaction was allowed to stir for 30 min whereupon DME (0.35 mL) was added. This resulted in the deposition of $LiI(DME)_2$ as a white solid. Storage at −25 °C for 24 h resulted in the further deposition of white solid. The solution was then filtered through a Celite column supported on glass wool (0.5 cm ×2 cm). The volatiles were then removed in vacuo, yielding a dark solid, which was subsequently dissolved in pentane (2 mL) to provide a dark brown yellow solution. Storage at −25 °C for 24 h resulted in the deposition of dark brown crystals, which were isolated by decanting off the supernatant (217 mg, 86% yield). Anal. Calcd for $MnN_4C_{36}H_{72}Li$: C, 69.42; H, 11.65; N, 8.99. Found: C, 69.31; H, 11.66; N, 9.13. ^1H NMR (C_6D_6, 25 °C, 500 MHz): δ 9.11 (br s, CMe_3). $^7Li\{^1H\}$ NMR (C_6D_6, 25 °C, 194 MHz): δ 85.3 (br, s). UV−vis (C_7H_8, 8.7×10^{-5} M): 323 nm ($\varepsilon = 9900$ L·mol^{-1}·cm^{-1}), 447 nm ($\varepsilon = 6800$ L·mol^{-1}·cm^{-1}), 521 nm ($\varepsilon = 2300$ L·mol^{-1}·cm^{-1}), 1003 nm ($\varepsilon = 480$ L·mol^{-1}·cm^{-1}). IR (hexane, cm^{-1}): 1615(s), 1617(s).

$[Li(12\text{-crown-}4)_2][Mn(N{=}C^tBu_2)_4]$ (3). To a brown yellow solution of **2** (64 mg, 0.102 mmol) in Et_2O (2 mL) was added a solution of 12-crown-4 (71 mg, 0.401 mmol) in pentane (3 mL). Storage at −25 °C for 24 h resulted in the deposition of a purple solid, which was isolated by decanting off the supernatant (93 mg, 94% yield). Anal. Calcd for $MnN_4C_{52}H_{104}O_8Li$: C, 64.04; H, 10.75; N, 5.74. Found: C, 63.66; H, 11.04; N, 5.35. ^1H NMR (pyridine-d_5, 25 °C, 500 MHz): δ 12.40 (br s, CMe_3), 3.66 (s, CH_2). $^7Li\{1H\}$ NMR: (C_6D_6, 25 °C, 194 MHz): δ 3.54 (s). UV−vis (DME, 5.8×10^{-5} M): 323 nm ($\varepsilon = 4000$ L·mol^{-1}·cm^{-1}), 403 nm ($\varepsilon = 3000$ L·mol^{-1}·cm^{-1}), 447 nm ($\varepsilon = 2300$ L·mol^{-1}·cm^{-1}), 541 nm ($\varepsilon = 790$ L·mol^{-1}·cm^{-1}), 904 nm ($\varepsilon = 550$ L·mol^{-1}·cm^{-1}). IR (DME, cm^{-1}): 1632(s).

$Mn(N{=}C^tBu_2)_4$ (4). To a yellow solution of **1** (371 mg, 0.479 mmol) in Et_2O (4 mL) was added I_2 (127 mg, 0.500 mmol) dissolved in Et_2O (2 mL). The solution immediately turned a dark red-orange. After stirring for 30 min the solution was stored at −25 °C for 24 h, resulting in the deposition of dark red-orange crystals, which were isolated by decanting off the supernatant (220 mg, 75% yield). Anal. Calcd for

$MnN_4C_{36}H_{72}$: C, 70.20; H, 11.78; N, 9.10. Found: C, 70.15; H, 12.13; N, 9.25. ^{1}H NMR (C_6D_6, 25 °C, 500 MHz): δ 5.10 (br s, CMe_3). UV−vis (C_7H_8, 9.8× 10^{-5} M): 332 nm (ε = 17300 L·mol^{-1}·cm^{-1}), 446 nm (ε = 12700 L·mol^{-1}·cm^{-1}), 520 nm (ε = 3900 L·mol^{-1}·cm^{-1}), 682 nm (ε = 1800 L·mol^{-1}·cm^{-1}). IR (hexane, cm^{-1}): 1617(s).

Cr(N═C^{t}Bu$_2$)$_4$ (5). To a white suspension of Li(N═C^{t}Bu$_2$) (493 mg, 3.35 mmol) in THF (3 mL) was added $CrCl_3$ (133 mg, 0.838 mmol). The solution immediately turned orange. This solution was allowed to stir for 20 min, whereupon I_2 (109 mg, 0.429 mmol) dissolved in Et_2O (2 mL) was added. The solution immediately darkened to red orange. Subsequent storage at −25 °C for 24 h resulted in the deposition of dark orange crystals, which were isolated by decanting off the supernatant (304 mg, 59% yield). Anal. Calcd for $CrN_4C_{36}H_{72}$: C, 70.54; H, 11.84; N, 9.14. Found: C, 70.23; H, 11.53; N, 9.28. ^{1}H NMR (C_6D_6, 25 °C, 500 MHz): δ 1.35 (s, CMe_3). ^{13}C{^{1}H} NMR (C_6D_6 25 °C, 125 MHz): δ 184.06 (N═C), 39.28 (CMe_3), 32.02 (Me). UV−vis (C_7H_8, 5.7× 10^{-5} M): 323 nm (ε = 34800 L·mol^{-1}·cm^{-1}), 521 nm (ε = 2000 L·mol^{-1}·cm^{-1}), 809 nm (ε = 1500 L·mol^{-1}·cm^{-1}). IR (hexane, cm^{-1}): 1581(m).

Mn$_3$(N═C^{t}Bu$_2$)$_6$ (6). *Method A.* A C_6D_6 (0.5 mL) solution of complex **4** (26 mg, 0.043 mmol) was heated at 50 °C for 6 h resulting in a color change to yellow-orange. The solvent was removed in vacuo yielding a dark yellow brown solid. Dissolution of the solid in hexanes (2 mL) and storage at −25 °C for 24 h resulted in the deposition of yellow-brown powder, which was isolated by decanting off the supernatant (7 mg, 49% yield). ^{1}H NMR (C_6D_6, 25 °C, 500 MHz): δ 17.16 (br s, CMe_3), 10.35 (br s, CMe_3).

Method B. To a white suspension of Li(N═C^{t}Bu$_2$) (134 mg, 0.912 mmol) in THF (2.5 mL) was added $MnCl_2$ (58 mg, 0.46 mmol). The solution immediately turned orange-red. This solution was allowed to stir for 1 h generating a deep orange solution. The solvent was removed in vacuo, and hexane (2 mL) was added to the resulting orange solid. The solution was then filtered through a Celite column supported on glass wool (0.5 cm ×2 cm), and the volume of the solution was reduced in vacuo to 1.5 mL. Storage at −25 °C for 24 h resulted in the deposition of orange cubes, which were isolated by decanting off the supernatant (76 mg, 50% yield). Calcd for $Mn_3N_6C_{54}H_{108}$: C, 64.45; H, 10.82; N, 8.35. Found: C, 64.18; H, 10.62; N, 8.28. ^{1}H NMR (C_6D_6, 25 °C, 500 MHz): δ 17.08 (br s, CMe_3), 10.24 (br s, CMe_3).

X-ray Crystallography. Data for **1**, **2**, **3**, **4**, and **6** were collected on a Bruker 3-axis platform diffractometer equipped with a SMART-1000 CCD detector using a graphite monochromator with a Mo Kα X-ray source (α = 0.71073 Å). The crystals were mounted on a glass fiber under Paratone-N oil and all data were collected at 150(2) K using an Oxford nitrogen gas cryostream system. A hemisphere of data was collected using ω scans with 0.3° frame widths. Frame exposures of 20, 30, 30, 15, and 25 s were used for complexes **1**, **2**, **3**, **4**, and **6**, respectively. Data collection and cell parameter determination were conducted using the SMART program.[79] Integration of the data frames and final cell parameter refinement were performed using SAINT software.[80] Absorption corrections were carried out empirically based on reflection ψ-scans. Subsequent calculations were carried out using SHELXTL.[81] Structure determination was done using direct or Patterson methods and difference Fourier techniques. All hydrogen atom positions were idealized, and rode on the atom of attachment. Structure solution, refinement, graphics, and creation of publication materials were performed using SHELXTL.[81] In complex **2**, the Li cation was found to be disordered over two sites and was modeled with half occupancy in each site. Alternate positions for the ketimide ligands were not observed. Additionally, for complex **4**, one *tert*-butyl group was found to be disordered between two positions about the tertiary carbon, in a 50:50 ratio. Idealized hydrogen atoms were not assigned to the disordered carbon atoms. A summary of relevant crystallographic data for **1**, **2**, **3**, **4**, and **6** is presented in Table 2.

■ ASSOCIATED CONTENT

Supporting Information. Cyclic voltammetry data for complexes **1**, **4**, and **5**. UV/vis spectra for **1**−**5**. X-ray crystallographic details (as CIF files), IR and NMR spectra for complexes **1**−**6**. This material is available free of charge via the Internet at http://pubs.acs.org.

■ AUTHOR INFORMATION

Corresponding Author
*E-mail: hayton@chem.ucsb.edu.

■ ACKNOWLEDGMENT

We thank the University of California, Santa Barbara for financial support of this work.

■ REFERENCES

(1) McEvoy, J. P.; Brudvig, G. W. *Chem. Rev.* **2006**, *106*, 4455–4483.
(2) Brudvig, G. W. *Phil. Trans. R. Soc. B* **2008**, *363*, 1211–1219.
(3) Yachandra, V. K.; Sauer, K.; Klein, M. P. *Chem. Rev.* **1996**, *96*, 2927–2950.
(4) Fukuzumi, S.; Kotani, H.; Prokop, K. A.; Goldberg, D. P. *J. Am. Chem. Soc.* **2011**, *133*, 1859–1869.
(5) Liu, W.; Groves, J. T. *J. Am. Chem. Soc.* **2010**, *132*, 12847–12849.
(6) Fukuzumi, S.; Fujioka, N.; Kotani, H.; Ohkubo, K.; Lee, Y.-M.; Nam, W. *J. Am. Chem. Soc.* **2009**, *131*, 17127–17134.
(7) Kumar, A.; Goldberg, I.; Botoshansky, M.; Buchman, Y.; Gross, Z. *J. Am. Chem. Soc.* **2010**, *132*, 15233–15245.
(8) Kim, S. H.; Park, H.; Seo, M. S.; Kubo, M.; Ogura, T.; Klajn, J.; Gryko, D. T.; Valentine, J. S.; Nam, W. *J. Am. Chem. Soc.* **2010**, *132*, 14030–14032.
(9) Song, W. J.; Seo, M. S.; DeBeer George, S.; Ohta, T.; Song, R.; Kang, M.-J.; Tosha, T.; Kitagawa, T.; Solomon, E. I.; Nam, W. *J. Am. Chem. Soc.* **2007**, *129*, 1268–1277.
(10) Charnock, J. M.; Garner, C. D.; Trautwein, A. X.; Bill, E.; Winkler, H.; Ayougou, K.; Mandon, D.; Weiss, R. *Angew. Chem., Int. Ed. Engl.* **1995**, *34*, 343–346.
(11) Camenzind, M. J.; Schardt, B. C.; Hill, C. L. *Inorg. Chem.* **1984**, *23*, 1984–1986.
(12) Jin, N.; Ibrahim, M.; Spiro, T. G.; Groves, J. T. *J. Am. Chem. Soc.* **2007**, *129*, 12416–12417.
(13) Mukherjee, C.; Weyhermüller, T.; Bothe, E.; Chaudhuri, P. *C. R. Chim.* **2007**, *10*, 313–325.
(14) Parsell, T. H.; Behan, R. K.; Green, M. T.; Hendrich, M. P.; Borovik, A. S. *J. Am. Chem. Soc.* **2006**, *128*, 8728–8729.
(15) Parsell, T. H.; Yang, M.-Y.; Borovik, A. S. *J. Am. Chem. Soc.* **2009**, *131*, 2762–2763.
(16) Gupta, R.; MacBeth, C. E.; Young, V. G.; Borovik, A. S. *J. Am. Chem. Soc.* **2002**, *124*, 1136–1137.
(17) MacBeth, C. E.; Gupta, R.; Mitchell-Koch, K. R.; Young, V. G.; Lushington, G. H.; Thompson, W. H.; Hendrich, M. P.; Borovik, A. S. *J. Am. Chem. Soc.* **2004**, *126*, 2556–2567.
(18) Shirin, Z.; Hammes, B. S.; Young, V. G.; Borovik, A. S. *J. Am. Chem. Soc.* **2000**, *122*, 1836–1837.
(19) Popescu, D. L.; Chanda, A.; Stadler, M.; de Oliveira, F. T.; Ryabov, A. D.; Munck, E.; Bominaar, E. L.; Collins, T. J. *Coord. Chem. Rev.* **2008**, *252*, 2050–2071.
(20) Miller, C. G.; Gordon-Wylie, S. W.; Horwitz, C. P.; Strazisar, S. A.; Peraino, D. K.; Clark, G. R.; Weintraub, S. T.; Collins, T. J. *J. Am. Chem. Soc.* **1998**, *120*, 11540–11541.
(21) Workman, J. M.; Powell, R. D.; Procyk, A. D.; Collins, T. J.; Bocian, D. F. *Inorg. Chem.* **1992**, *31*, 1548–1550.
(22) Collins, T. J.; Powell, R. D.; Slebodnick, C.; Uffelman, E. S. *J. Am. Chem. Soc.* **1990**, *112*, 899–901.

(23) Collins, T. J.; Gordonwylie, S. W. *J. Am. Chem. Soc.* **1989**, *111*, 4511–4513.
(24) MacDonnell, F. M.; Fackler, N. L. P.; Stern, C.; O'Halloran, T. V. *J. Am. Chem. Soc.* **1994**, *116*, 7431–7432.
(25) Fallis, I. A.; Farrugia, L. J.; Macdonald, N. M.; Peacock, R. D. *Dalton Trans.* **1993**, 2759–2763.
(26) Yiu, S.-M.; Lam, W. W. Y.; Ho, C.-M.; Lau, T.-C. *J. Am. Chem. Soc.* **2007**, *129*, 803–809.
(27) Du Bois, J.; Tomooka, C. S.; Hong, J.; Carreira, E. M. *Acc. Chem. Res.* **1997**, *30*, 364–372.
(28) Kessissoglou, D. P.; Li, X.; Butler, W. M.; Pecoraro, V. L. *Inorg. Chem.* **1987**, *26*, 2487–2492.
(29) Kurahashi, T.; Kikuchi, A.; Shiro, Y.; Hada, M.; Fujii, H. *Inorg. Chem.* **2010**, *49*, 6664–6672.
(30) Gohdes, J. W.; Armstrong, W. H. *Inorg. Chem.* **1992**, *31*, 368–373.
(31) Larson, E.; Lah, M. S.; Li, X.; Bonadies, J. A.; Pecoraro, V. L. *Inorg. Chem.* **1992**, *31*, 373–378.
(32) Bower, B. K.; Tennent, H. G. *J. Am. Chem. Soc.* **1972**, *94*, 2512–2514.
(33) Lappert, M.; Protchenko, A.; Power, P. P.; Seeber, A. *Metal Amide Chemistry*; John Wiley & Sons: West Sussex, U.K., 2009.
(34) Bradley, D. C.; Mehrotra, R. C.; Rothwell, I. P.; Singh, A. *Alkoxo and Aryloxo Derivatives of Metals*; Academic Press: London, U.K., 2001.
(35) Lewis, R. A.; Wu, G.; Hayton, T. W. *J. Am. Chem. Soc.* **2010**, *132*, 12814–12816.
(36) Soriaga, R. A. D.; Nguyen, J. M.; Albright, T. A.; Hoffman, D. M. *J. Am. Chem. Soc.* **2010**, *132*, 18014–18016.
(37) Murray, B. D.; Power, P. P. *Inorg. Chem.* **1984**, *23*, 4584–4588.
(38) Nakamoto, M.; Fukawa, T.; Lee, V. Y.; Sekiguchi, A. *J. Am. Chem. Soc.* **2002**, *124*, 15160–15161.
(39) Boudreaux, E. A.; Mulay, L. N. *Theory and Applications of Molecular Paramagnetism*; John Wiley & Sons: New York, 1976.
(40) Shearer, H. M. M.; Snaith, R.; Sowerby, J. D.; Wade, K. *Chem. Commun.* **1971**, 1275–1276.
(41) Cirera, J.; Ruiz, E.; Alvarez, S. *Inorg. Chem.* **2008**, *47*, 2871–2889.
(42) Edema, J. J. H.; Gambarotta, S.; van Bolhuis, F.; J.J. Smeets, W.; Spek, A. L.; Chiang, M. Y. *J. Organomet. Chem.* **1990**, *389*, 47–59.
(43) Hao, S.; Gambarotta, S.; Bensimon, C. *J. Am. Chem. Soc.* **1992**, *114*, 3556–3557.
(44) Morris, R. J.; Girolami, G. S. *Organometallics* **1991**, *10*, 792–799.
(45) Witten, E. H.; Reiff, W. M. *Inorg. Chim. Acta* **1980**, *41*, 227–228.
(46) Goodwin, H. A.; Sylva, R. S. *Aust. J. Chem.* **1967**, *20*, 629–637.
(47) Lewis, J.; Nyholm, R. S.; Smith, P. W. *J. Chem. Soc.* **1961**, 4590–4599.
(48) Yang, L.; Powell, D. R.; Houser, R. P. *Dalton Trans.* **2007**, 955–964.
(49) Krishnamurthy, R.; Schaap, W. B. *J. Chem. Educ.* **1969**, *46*, 799.
(50) Morris, R. J.; Girolami, G. S. *Organometallics* **1989**, *8*, 1478–1485.
(51) Martins, A. M.; Marques, M. M.; Ascenso, J. R.; Dias, A. R.; Duarte, M. T.; Fernandes, A. C.; Fernandes, S.; Ferreira, M. J.; Matos, I.; Conceição Oliveira, M.; Rodrigues, S. S.; Wilson, C. *J. Organomet. Chem.* **2005**, *690*, 874–884.
(52) Cotton, F. A.; Wilkinson, G. *Advanced Inorganic Chemistry*, 6th ed.; John Wiley & Sons: New York, 1999.
(53) Brunner, H.; Koch, H. *Chem. Ber.* **1982**, *115*, 65–83.
(54) Yur'eva, L. P.; Peregudova, S. M.; Nekrasov, L. N.; Korotkov, A. P.; Zaitseva, N. N.; Zakurin, N. V.; Vasil'kov, A. Y. *J. Organomet. Chem.* **1981**, *219*, 43–51.
(55) Liu, J. S.-Y.; Chen, P.-Y.; Sun, I.-W.; Hussey, C. L. *J. Electrochem. Soc.* **1997**, *144*, 2388–2392.
(56) Schulzke, C.; Enright, D.; Sugiyama, H.; LeBlanc, G.; Gambarotta, S.; Yap, G. P. A.; Thompson, L. K.; Wilson, D. R.; Duchateau, R. *Organometallics* **2002**, *21*, 3810–3816.
(57) Murray, B. D.; Hope, H.; Power, P. P. *J. Am. Chem. Soc.* **1985**, *107*, 169–173.
(58) Budzichowski, T. A.; Chisholm, M. H.; Strieb, W. E. *J. Am. Chem. Soc.* **1994**, *116*, 389–390.
(59) Warkentin, J.; Hine, K. F. *Can. J. Chem.* **1970**, *48*, 3545–3548.
(60) de Haan, J. W.; van de Ven, L. J. M.; Wilson, A. R. N.; van der Hout-Lodder, A. E.; Altona, C.; Faber, D. H. *Org. Magn. Res.* **1976**, *8*, 477–482.
(61) Pitkänen, M.; Laihia, K.; Schulze, K. *Org. Magn. Reson.* **1984**, *22*, 543–546.
(62) Campbell, J. A.; McDougald, G.; McNab, H.; Rees, L. V. C.; Tyas, R. G. *Synthesis* **2007**, 3179–3184.
(63) Birrell, R. N.; Trotman-Dickenson, A. F. *J. Chem. Soc.* **1960**, 4218–4224.
(64) Metcalfe, E. L. *J. Chem. Soc.* **1963**, 3560–3567.
(65) Costello, A. R.; Smith, J. R. L.; Stark, M. S.; Waddington, D. J. *Faraday Trans.* **1996**, *92*, 3497–3507.
(66) Hioe, J.; Zipse, H. *Org. Biomol. Chem.* **2010**, *8*, 3609–3617.
(67) Kiplinger, J. L.; Morris, D. E.; Scott, B. L.; Burns, C. J. *Organometallics* **2002**, *21*, 3073–3075.
(68) Ferreira, M. J.; Matos, I.; Ascenso, J. R.; Duarte, M. T.; Marques, M. M.; Wilson, C.; Martins, A. M. *Organometallics* **2007**, *26*, 119–127.
(69) Ferreira, M. J.; Martins, A. M. *Coord. Chem. Rev.* **2006**, *250*, 118–132.
(70) Yamada, J.; Fujiki, M.; Nomura, K. *Organometallics* **2005**, *24*, 2248–2250.
(71) Morton, A. A.; Stevens, J. R. *J. Am. Chem. Soc.* **1931**, *53*, 2769–2772.
(72) Love, B. E.; Tsai, L. *Synth. Commun.* **1992**, *22*, 3101–3108.
(73) Kauffmann, T.; Albrecht, J.; Berger, D.; Legler, J. *Angew. Chem., Int. Ed. Engl.* **1967**, *6*, 633–634.
(74) Armstrong, D. R.; Barr, D.; Snaith, R.; Clegg, W.; Mulvey, R. E.; Wade, K.; Reed, D. *Dalton Trans.* **1987**, 1071–1081.
(75) Clegg, W.; Snaith, R.; Shearer, H. M. M.; Wade, K.; Whitehead, G. *Dalton Trans.* **1983**, 1309–1317.
(76) Jennings, J. R.; Snaith, R.; Mahmoud, M. M.; Wallwork, S. C.; Bryan, S. J.; Halfpenny, J.; Petch, E. P.; Wade, K. *J. Organomet. Chem.* **1983**, *249*, c1–c5.
(77) Evans, D. F. *J. Chem. Soc.* **1959**, 2003–2005.
(78) Bain, G. A.; Berry, J. F. *J. Chem. Educ.* **2008**, *85*, 532–536.
(79) *SMART Software Users Guide*, 5.1; Bruker Analytical X-Ray Systems, Inc: Madison, WI, 1999.
(80) *SAINT Software Users Guide*, 5.1; Bruker Analytical X-Ray Systems, Inc: Madison, WI, 1999.
(81) Sheldrick, G. M. *SHELXTL*, 6.12; Bruker Analytical X-Ray Systems, Inc: Madison, WI, 2001.